ANALYSIS OF MODE LOCALIZATION IN A SINGLE-LAYER SPHERICAL RETICULATED SHELL

Z. H. Liu – W. Liu – W. C. Gao[*] – X. Cheng

Department of Astronautic Science and Mechanics, Harbin Institute of Technology, Harbin 150001, China

Abstract:

The occurrence of the mode localization is studied in a structure of a single-layer spherical reticulated shell. The matrix perturbation method is used to analyze the mechanism of the occurrence of mode localization. The dynamical characteristics of this structure, especially the effects of the variation of the stiffness parameter on the vibration modes of the structure, were analyzed by numerical simulations. An amplitude significance coefficient is proposed as a measure of the degree of the mode localization. The results show that small deviations of the stiffness parameter can cause significant changes to the structural dynamics characteristics; the mode localization does occur for some particular modes of this structure in the case of random stiffness mistuning. Preliminary analysis found that the mode can be considered as strongly localized when the amplitude significance coefficient is greater than 8.

1 Introduction

The mode localization phenomenon in the mistuned periodic structure with cyclic symmetry has been heavily studied in the past few decades. The phenomenon was first observed by Anderson and Mott in their research to explain the transport properties of disordered solids in 1958 [1]. Early studies were devoted to investigate the electrical conduction processes in disordered solids. In solid state physics, mode localization typically means that the state vector associated with a particle becomes localized to a small region, and the probability of finding the particle outside this region becomes infinitely small; thus, the particle becomes "trapped" and an "ordered" solid may change from a metallic conductor to a semiconductor [2]. Similar to the mode localization phenomenon in solid state physics, in the vibration problems encountered in

structural dynamics, the mistuning of periodic structures may localize the vibration modes and confine the energy to a region close to the source. Therefore, a lot of research work was done in the 1980s on periodic structures and the mode localization analysis is extended to the field of structural vibration [3-5].

A large number of theoretical and experimental studies on the mode localization phenomenon have been reported during the past few decades. These research studies mainly focused on periodic structures with cyclic symmetry [2-9], such as bladed disk in turbo machines, flexible space antennas, large astronomical telescope, and so on. Previous studies showed that the dynamic characteristics of the structures could be radically different from their ideal values owing to small deviations, such as manufacturing or construction errors, geometrical irregularity, material defects and

[*] Corresponding author. Tel.0086-(0)451-86402713; fax:0086-(0)451-86402713
*E-mail address:*gaoweicheng@sina.com

structural damage, etc. Using their ideal values as the structural responses these studies would lead to completely erroneous results. The analysis of mode localization in one-dimensional linear and nonlinear lattices showed that the analysis of the linear problems was a necessary step for the transition to the nonlinear ones [10]. The reticulated shell, which usually has elegant designs, is an architecture structure with many applications. Nowadays, reticulated shells, especially spherical reticulated shells have been heavily studied and widely used [11-13]. As one of the periodic structures with cyclic symmetry, spherical reticulated shell structures also consist of many identical or similar member bars; however, to our knowledge, little work has been devoted to the analysis of the mode localization in them.

Considering the structural similarity of the spherical reticulated shell structure with the bladed disk in turbo machines and flexible space antennas, we studied the occurrence of the mode localization in a single-layer spherical reticulated shell model. The paper is laid out as follows: in the first section of the paper, the occurrence mechanism of the mode localization phenomenon is analyzed with the matrix perturbation method; in the second section, the occurrence of the mode localization is studied by FEM simulation in a single-layer spherical reticulated shell. The effect of the random stiffness mistuning parameters on the natural frequencies and the mode shapes are analyzed. Subsequently, the mode shape characteristics of the structure under different mistuning parameters are analyzed, and an amplitude significance coefficient is proposed as a measure of the degree of the mode localization. In the end, the main results of this paper are summarized, and the prospective research is suggested.

2   Mechanism of localization phenomenon

When the structural stiffness matrix or mass matrix has small changes, matrix perturbation method is undoubtedly a powerful tool of structure re-analysis. The basic idea of the perturbation method is using the eigenvalues and eigenvectors of the structural state without any mistuning to approximately express the structural state of the mistuned structure [14]. Here, the matrix perturbation method is used to study the occurrence mechanism of localization vibration in a mistuned single-layer spherical reticulate shell structure.

For an undamped system, the free vibration eigenvalue problem is given by

$$\mathbf{Ku} = \lambda \mathbf{Mu} , \qquad (1)$$

where, $\mathbf{K}$ and $\mathbf{M}$ are the stiffness matrix and the mass matrix, respectively, λ denotes the eigenvalue, and $\mathbf{u}$ is the modal vector. When a small perturbation is introduced, the mass matrix and stiffness matrix can be described as:

$$\mathbf{M} = \mathbf{M_0} + \varepsilon \mathbf{M_1} , \qquad (2)$$
$$\mathbf{K} = \mathbf{K_0} + \varepsilon \mathbf{K_1} , \qquad (3)$$

where ε is a parameter representing the disorder in the system. Thus, $\varepsilon \mathbf{K_1}$ is a variation of the unperturbed stiffness matrix $\mathbf{K_0}$, and $\varepsilon \mathbf{M_1}$ is a variation of the unperturbed mass matrix $\mathbf{M_0}$. The perturbation matrices $\mathbf{K_1}$ and $\mathbf{M_1}$ are of the same order as the unperturbed matrices.

According to the perturbation theory, the eigenvectors and eigenvalues can be expanded in a power series, i.e.,

$$\lambda_i = \lambda_{0i} + \varepsilon \lambda_{1i} + \varepsilon^2 \lambda_{2i} + \dots , \qquad (4)$$
$$\mathbf{u}_i = \mathbf{u}_{0i} + \varepsilon \mathbf{u}_{1i} + \varepsilon^2 \mathbf{u}_{2i} + \dots , \qquad (5)$$

Substituting Eqs (2), (3), (4) and (5) into (1), and comparing the coefficient of the first power of ε, the following result can be obtained,

$$\mathbf{K_0} \mathbf{u}_{1i} + \mathbf{K_1} \mathbf{u}_{0i} = \lambda_{0i} \mathbf{M_0} \mathbf{u}_{1i} + \lambda_{0i} \mathbf{M_1} \mathbf{u}_{0i} + \lambda_{1i} \mathbf{M_0} \mathbf{u}_{0i} . \qquad (6)$$

The expansion theorem states that any nonzero vector can be expressed as a linear combination of n of independent vectors. Thus, $\mathbf{u}_{1i}$ can be written as

$$\mathbf{u}_{1i} = \sum_{s=1}^{n} C_{1s} \mathbf{u}_{0s} . \qquad (7)$$

Substituting Eq. (7) into (6), and premultiplying the resulting equations by the transpose of $\mathbf{u}_{0s}$ to obtain

$$\mathbf{u}_{0s}{}^T \mathbf{K_0} \sum_{s=1}^{n} C_{1s} \mathbf{u}_{0s} + \mathbf{u}_{0s}{}^T \mathbf{K_1} \mathbf{u}_{0i} =$$
$$\mathbf{u}_{0s}{}^T \left(\lambda_{1i} \mathbf{M_0} \mathbf{u}_{0i} + \lambda_{0i} \mathbf{M_0} \sum_{s=1}^{n} C_{1s} \mathbf{u}_{0s} + \lambda_{0i} \mathbf{M_1} \mathbf{u}_{0i} \right) . \qquad (8)$$

Considering the orthogonality conditions:

$$\mathbf{u}_{0i}^T \mathbf{M}_0 \mathbf{u}_{0j} = \delta_{ij} \qquad (i,j = 1 \sim n), \qquad (9)$$

where δ_{ij} is the Kronecker symbol, we obtain,

$$C_{1s}(\lambda_{0i} - \lambda_{0s}) + \lambda_{1i}\delta_{is} = \mathbf{u}_{0s}^T \mathbf{K_1} \mathbf{u}_{0i} - \lambda_{0i}\mathbf{u}_{0s}^T \mathbf{M_1}\mathbf{u}_{0i}. \qquad (10)$$

If $i \neq s$, $\delta_{is} = 0$, C_{1s} can be obtained from Eq. (10),

$$C_{1s} = \frac{1}{\lambda_{0i} - \lambda_{0s}} \mathbf{u}_{0s}^T (\mathbf{K_1} - \lambda_{0i}\mathbf{M_1})\mathbf{u}_{0i}. \qquad (11)$$

If $i = s$, C_{1i} is determined from the normalization condition,

$$C_{1i} = -\frac{1}{2}\mathbf{u}_{0i}^T \mathbf{M_1}\mathbf{u}_{0i}. \qquad (12)$$

Substituting Eqs (10), (11) into (7), the first-order perturbation of the eigenvectors can be written as

$$\mathbf{u}_{1i} = \sum_{s=1, s \neq i}^{n} \frac{1}{\lambda_{0i} - \lambda_{0s}} \left[\mathbf{u}_{0s}^T (\mathbf{K_1} - \lambda_{0i}\mathbf{M_1})\mathbf{u}_{0i} \right] \mathbf{u}_{0s}$$
$$- \frac{1}{2}\left(\mathbf{u}_{0s}^T \mathbf{M_1}\mathbf{u}_{0s} \right)\mathbf{u}_{0s}. \qquad (13)$$

As shown in Eq.(13), the eigenvectors $\mathbf{u}_{1i}$ are determined by the following factors: 1) the eigenvalues λ_{0i} and eigenvectors $\mathbf{u}_{0i}$; 2) the first-order perturbation of mass matrix and stiffness matrix ($\mathbf{M}_1$ and $\mathbf{K}_1$). The eigenvalues λ_{0i} and eigenvectors $\mathbf{u}_{0i}$ are determined by the structural characteristics of the original system. When the difference of unperturbed frequencies is small, the denominator $\lambda_{0i} - \lambda_{0s}$ is a very small number. Then the first-order perturbation of the eigenvectors $\mathbf{u}_{1i}$ is very large. The cumulative effect over n terms can then produce $\varepsilon\mathbf{u}_{1i}$ is no longer the first order of

eigenvectors, as expected. A single-layer spherical reticulated shell structure is a physical system with high modal densities. A small change of structural parameters may result in that the eigenvectors change remarkably suffering strong mode localization.

3 Modal analysis

3.1 Numerical simulation

The finite element approach is an important method for the vibration analysis of almost any complex engineering structure [15]. In this subsection, a single-layer spherical reticulated shell structure is considered and the mode localization phenomenon is discussed. The geometry of the reticulated shell structure is shown in Fig. 1. It consists of a number of circumferential ribs and longitudinal ribs. The geometric parameters and material parameters of the single-layer spherical reticulated shell are shown in Table 1 and Table 2, respectively.
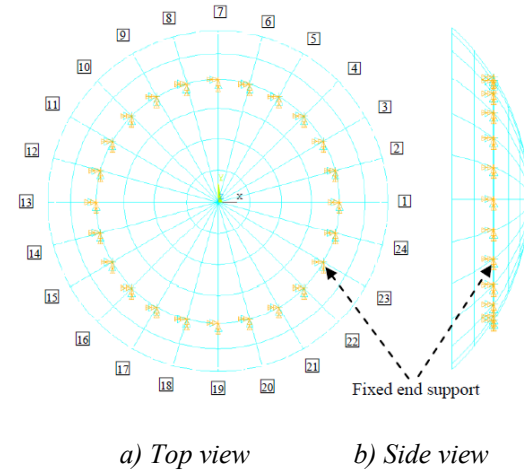

a) Top view   *b) Side view*

Figure 1. Schematic diagram of the single-layer spherical reticulated shell.

Table 1. Geometric parameters of the single-layer spherical reticulated shell.

Spherical radius [m]	Height [m]	Span [m]	Sector-Number	Circular-Number
19.95	6.8	30	24	6

Table 2. Material parameters of the single-layer spherical reticulated shell.

Material	Density ρ [kg·m⁻³]	Elastic modulus E [MPa]	Poisson ratio μ	Yield strength σ_s [MPa]

Q235	7850	2.06×10^5	0.3	235

All the ribs are circular steel tubes with the following cross-section sizes: ϕ 159×8 for longitudinal ribs; ϕ 63.5×3 for circumferential ribs. All the ribs are treated as Beam188 elements which are defined in ANSYS. They are linear, or quadratic, or cubic two-node beam elements in 3-D. The element is based on the beam theory of Timoshenko which includes shear-deformation effects. It is suitable for analyzing slender to moderately stubby or thick beam structures. In the computational model, the nodes at which the fourth ring and the radial ribs intersect are treated as fixed ends as the marking shown in Fig. 1.

In order to illustrate the effects of structural imperfections on the dynamic characteristics of the structure, the stiffness mistuning was introduced into the 24 sets of longitudinal ribs by altering their stiffness K (in Fig. 2) by an amount of $\Delta K/K$.
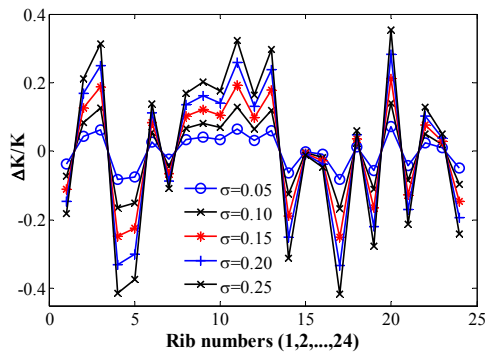

Figure 2. Specific distribution of the stiffness mistuning of 24 sets of longitudinal ribs.

Here, $\Delta K/K$ is a group of normally distributed random numbers with a mean of 0 and a standard deviation of σ. The serial numbers of the 24 sets of longitudinal ribs are shown in Fig. 1. The specific distribution of the stiffness mistuning used in generating the results in this work is shown in Fig. 2. The mode characteristics of the single-layer spherical reticulated shell were analyzed using FEA software-ANSYS. The natural frequencies and mode shapes are the important dynamic characteristics of structural systems, so the natural

frequencies of the first fifty modes are extracted and their respective vibration mode shapes are analyzed.

3.2 Results and discussion

3.2.1   Frequency comparison of the tuned and mistuned structure

In numerical simulations, the natural frequencies of the first fifty modes were extracted from both the tuned and mistuned models. The natural frequency comparisons of the first fifty modes between the tuned and mistuned structures are plotted in Fig.3. Due to space limitations, only the calculation results of the first ten order frequencies are listed in Table 3, where $\sigma = 0$ and $\sigma = 0.25$ represent the standard deviation of the stiffness mistuning parameters of the tuned and mistuned structures, respectively.

As shown in Fig. 3, the first fifty order frequencies of the tuned and mistuned structures are intensive. The frequency difference between the tuned and mistuned structures is not obvious. The low frequencies of the tuned and mistuned structure are almost the same, which indicates that the small stiffness mistuning has minimal impacts on the natural frequencies of the structure.
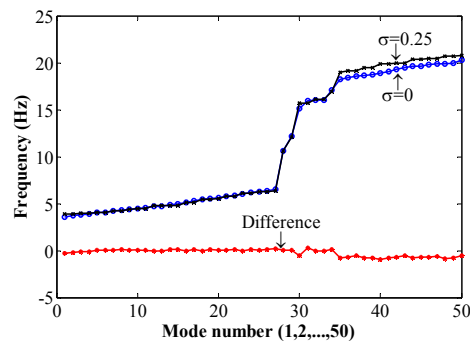

Figure 3. Natural frequency comparison of the first fifty modes between the tuned and mistuned structure.

In Table 3, there are repetitive frequency features in the first ten orders of the natural frequencies when $\sigma = 0$, i.e., in the tuned structure.

Table 3. First ten order frequencies of the tuned and mistuned structure.

Frequency	Mode									
[Hz]	1st	2nd	3rd	4th	5th	6th	7th	8th	9th	10th

σ=0	3.915	3.915	3.970	3.970	4.023	4.023	4.215	4.215	4.350	4.470
σ=0.25	3.604	3.720	3.839	3.877	4.038	4.096	4.221	4.340	4.410	4.480
Difference	-0.311	-0.196	-0.131	-0.093	0.015	0.073	0.006	0.124	0.060	0.010

It can be seen that the first four pairs of data, i.e., those of the 1st and 2nd order, the 3rd and 4th order, the 5th and 6th order, the 7th and 8th order, are equal, respectively. The repetitive frequency of the tuned structure degenerates into two adjacent frequencies when σ = 0.25, i.e., in the mistuned structure.

3.2.2 Mode comparison of the tuned and mistuned structure

This system has very high modal densities. Previous studies showed that the dynamic system with close eigenvalues was likely to cause the occurrence of mode localization [3-11]. In order to study the characteristic of the mode shape of the structure, we extract the contour of displacement vector sums (DVSs) of the first four modes of the tuned and mistuned structure. It can seem from Fig. 4 and Fig. 5 that the vibration of the first four modes of the structure is mainly concentrated in the outer ring bars.

For a more detailed quantitative analysis of the calculated results, the modal displacements are normalized by the maximum DVS of the end-nodes of the 24 sets of the longitudinal ribs in the mistuned structure. The comparisons of the normalized amplitudes of the end-nodes between the tuned and mistuned structure are plotted in Fig. 6. The vibrations of the first four modes of the tuned structure are relatively uniform and have a regular form. The vibration of the mistuned structure is confined to very few longitudinal ribs of the structure, and the vibration displacements of the other ribs are almost zero, thus the mode is localized. When σ = 0, the variation of the normalized amplitudes of the rib end-nodes resembles a sinusoidal wave (Figs. 6a–d). This is determined by the periodicity of a single-layer spherical reticulated shell structure. As the distribution of the modal vibration energy is relatively uniform, the normalized amplitudes of the rib end-nodes of the

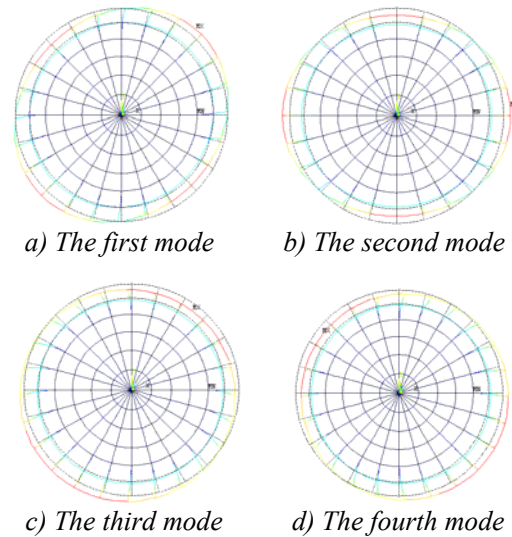24 sets of the longitudinal ribs are the tuned form of a trigonometric curve.

a) The first mode   *b) The second mode*

c) The third mode   *d) The fourth mode*

Figure 4. Contour of normalized amplitudes of the first four modes of tuned structure.

a) The first mode   *b) The second mode*

c) The third mode   *d) The fourth mode*
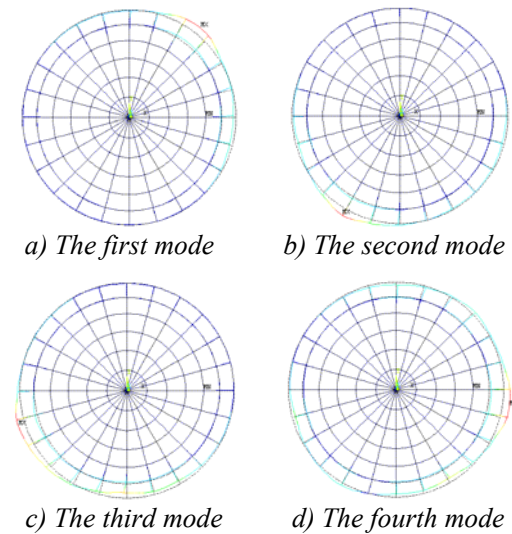
Figure 5. Contour of DVSs of the first four modes of the mistuned structure.

a) The first mode

b) The second mode
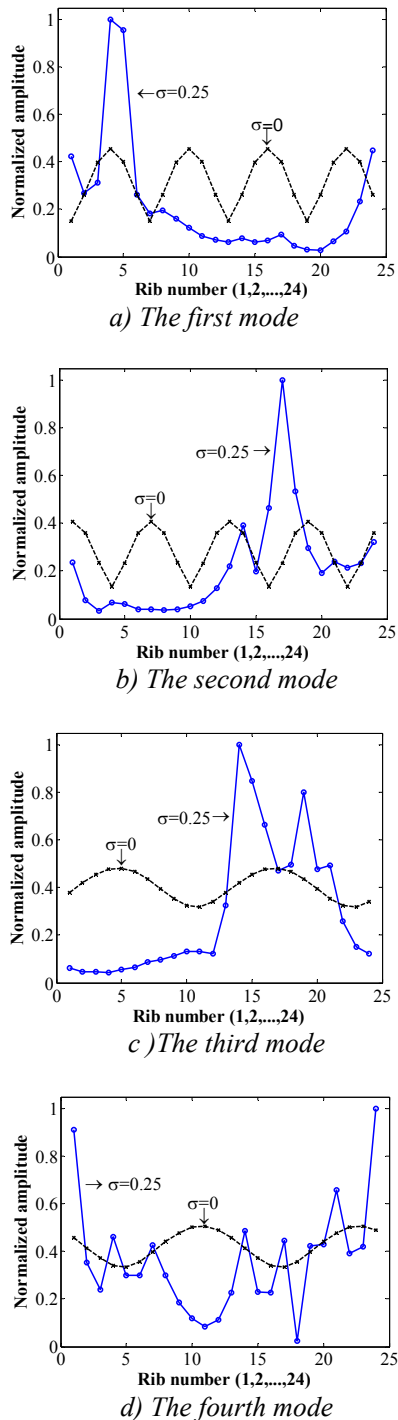

c)The third mode

d) The fourth mode

Figure 6. Comparison of the normalized amplitude of the first four modes between the tuned and mistuned structure.

When σ =0.25, the first four modes are different compared with those of the tuned structure. The first order vibration is only confined to the 4th and the

5th sets of longitudinal ribs, the normalized amplitudes of the two rib end-nodes are 2.20 times and 2.38 times of that order of the tuned structure, respectively.

Most of the normalized amplitudes of the other rib end-nodes are lower than the one-fifth of the maximum value, the localized effect of the first order is obvious (Fig. 6a). Although the second order and the third order modes of the mistuned structure have not such great change as the first order, more than half numbers of the normalized amplitudes of the two modes are still lower than the one-fifth of the maximum value. For the second order mode, the vibration is mainly confined to the 16th to the 18th sets of longitudinal ribs. The normalized amplitude of the 17th sets of longitudinal ribs is the maximum one, and it is 4.27 times of that of the tuned structure (Fig. 6b). For the third mode, the maximum normalized amplitude of the mistuned structure is 2.37 times of that of the tuned structure (Fig. 6c). The fourth order modal shape of the mistuned structure has changes compared with the tuned structure, but the vibration is considered to be extended, all the nodes have different levels of vibration, their normalized amplitudes are greater than the one-fourth of the maximum value. The maximum normalized amplitude of the mistuned structure is 2.04 times of that of the tuned structure (Fig. 6d). The localized effect of the first order is the most obvious in the former four modes. It was found out that the mode localization phenomenon also occurs in some higher order modes of the first fifty modes. Note that the different modes typically localize at different sets of ribs, the locations of the maximum normalized amplitude cannot be anticipated from a cursory inspection of the actual distribution of random mistuning, Fig. 2.

As shown in Figs. 6a–d, the normalized amplitudes of the rib end-nodes of the first four modes of the mistuned structure have a great change compared with those of the tuned structure, and they no longer have the tuned form of trigonometric curves. We selected the normalized amplitudes of the rib end-nodes for the first four modes in the tuned and mistuned structure as sample space. The amplitude standard deviations of the sample spaces were calculated to describe the dispersion of the rib end-nodes of the longitudinal ribs in the tuned and mistuned structure, respectively. The formula of standard deviation is written as:

$$\sigma_{d(u)} = \sqrt{\frac{1}{N} \sum_{j=1}^{n} (p_j - \overline{p})} , \qquad (14)$$

where p_j is the normalized amplitude of the j-th set of longitudinal ribs (j=1, 2…, 24), $\overline{p}$ is the mean of the normalized amplitudes of the 24 sets of longitudinal ribs. σ_u and σ_d represents the amplitude standard deviation of normalized amplitudes of the tuned and mistuned structure, respectively.

As can be seen from Table 4, in the tuned structure, the amplitude standard deviations σ_u of the first two modes are equal to 3.286×10^{-4}; those of the third and fourth order modes are equal to 1.492×10^{-4}. Previous analysis shows that the frequencies of the 1st and 2nd order, 3rd and 4th order are equal, respectively (Table 3). This shows that there is a correspondence between the frequencies and mode shapes. When mode localization occurs, the vibration energy is confined to a few ribs, the amplitude of vibration of these ribs increases, while that of the other ribs reduces correspondingly. As shown in Table 4, the standard deviation σ_d of the first four modes becomes larger compared with σ_u. It reflects that the first four modes have changed greatly compared with the tuned structure and the vibration energy is no longer uniformly distributed from one aspect.

Table 4. Amplitude standard deviation.

| Amplitude standard deviation	Mode			
	1st ($\times 10^{-4}$)	2nd ($\times 10^{-4}$)	3rd ($\times 10^{-4}$)	4th ($\times 10^{-4}$)
σ_u	3.286	3.286	1.492	1.492
σ_d	7.977	7.470	7.336	5.661

3.2.3   Results with different stiffness mistuning parameters

It is clear that from the results above, the strong mode localization does occur in the first three modes when σ is equal to 0.25. When σ changes from 0.05 to 0.25, the variations of the modal displacement with the rib number for the first four modes of the structure are plotted in Fig. 7.
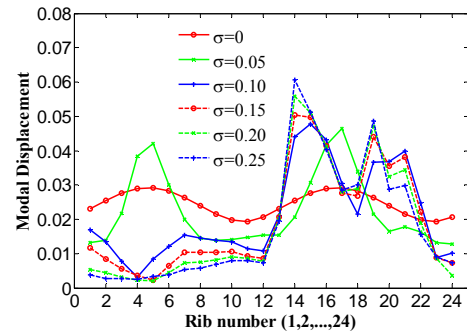
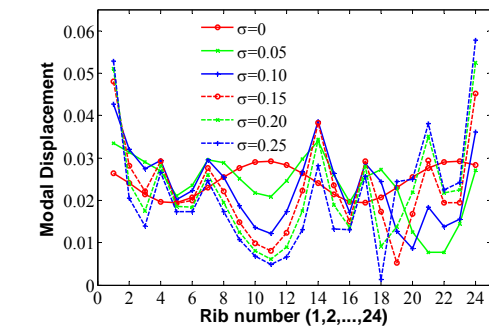The modal mass matrix is independent of the stiffness mistuning parameters.
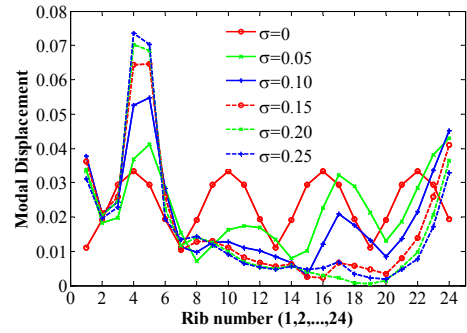
a) The first mode
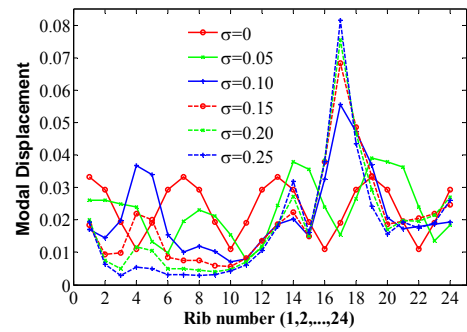
b) The second mode

c) The third mode

d) The fourth mode

Figure 7. Variations of the modal displacement with the rib number for the first four modes of the structure.

Modal displacements obtained in software are normalized with respect to the same mass matrix, so they are comparable. When σ varies from 0.15 to 0.25, the localized phenomenon of the first three modes is relatively more obvious. The vibration of the mistuned structure is confined to very few longitudinal ribs of the structure, the modal displacements of more than half numbers of the longitudinal ribs are less than 0.01. The localized phenomenon of the fourth mode is not obvious compared with the former three modes. When σ are equal to 0.05 and 0.10, the mode shapes of the first four modes are similar to those of the tuned structure and the mode localization is not obvious for all the former four modes. As the standard deviation σ decreases from 0.05 to 0.25, the maximum modal displacement is increased but the modal displacements of the other longitudinal ribs are decreased as shown in Figs. 7 a) – d).

3.2.4   Amplitude significance coefficient

For the purpose of discussing the results of numerical experiments and comparing the degree of mode localization of different modes, the amplitude significance coefficient R_i is proposed here.
For the i-th mode, the corresponding amplitude significance coefficient is

$$R_i = (P_{imax} - M_{i2/3}) / M_{i2/3} , \qquad (15)$$

where P_{imax} is the maximum modal displacements of all the longitudinal rib end-nodes for the ith mode of the mistuned structure, $M_{i2/3}$ is the mean of the first two-thirds of the minimum modal displacements of the longitudinal rib end-nodes for the i-th mode of the mistuned structure, respectively.
According to the above conclusion of the contour of DVS, the degree of the mode localization of the first mode is the most obvious. As shown in Fig. 8, the amplitude significance coefficient R_i of the first mode is also greater than that of the other three modes when the standard deviation of mistuning parameters is equal to 0.25. The greater the amplitude significance coefficient R_i, the stronger the degree of the mode localization. It indicates that the amplitude significance coefficient denotes that the degree of the mode localization is sound.
As the mode number increases, the amplitude significance coefficient gradually becomes smaller in Fig.8. It indicates that the degree of the mode

localization of lower mode is more obvious than that of higher order modes in our model of this single-layer spherical reticulated shell structure. When σ = 0.25, the above analysis of subsection 3.2.2 shows that the localized phenomenon of the first three modes is relatively more obvious and in Fig.8 the amplitude significance coefficient R_i of the first three modes is greater than 8. For the fourth order mode, the mode localization phenomenon was not obvious and the amplitude significance coefficient R_i was smaller than 8. Preliminary analysis found that the mode can be considered as strongly localized when the amplitude significance coefficient is greater than 8. Once this critical value has been given, checking the degree of the mode localization phenomenon becomes easy. When the stiffness mistuning parameters vary with the standard deviation from 0.05 to 0.25, not every order mode is strongly localized. Due to limited space, the corresponding contour of DVSs of the mistuned structure is here no longer given.
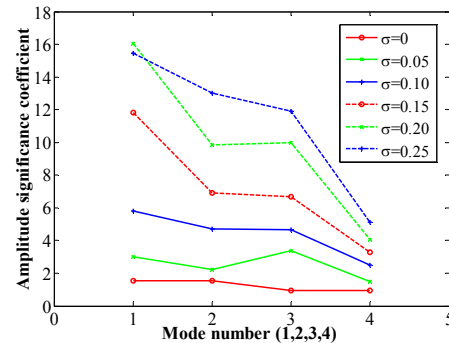

Figure 8. Curve of amplitude significance coefficient.

4   Conclusions

In this paper, the mode localization of a single-layer spherical reticulated shell has been studied with the matrix perturbation method and FEM simulations. The conclusions are summarized as follows:
1) The analysis of the matrix perturbation method indicated that a slight variation of the stiffness matrix or mass matrix can cause the eigenvectors of closely spaced modes to change remarkably, leading to the mode localization phenomenon.
2) The results of numerical simulation prove that the mode localization can occur in some particular mode of the mistuned single-layer spherical reticulated shell. As the mistuning

parameter amplitude increases, the maximum modal displacement of the longitudinal rib end-nodes becomes correspondingly larger.

3) The proposed amplitude significance coefficient R_i can effectively describe the degree of the mode localization.

4) The results indicate that the localized phenomenon of lower order modes is more evident than that of higher order modes and not every mode has discernable mode localization phenomenon. Our analysis found that the mode could be considered as localized when $R_i > 8$.

Currently, mode localization is still a research area not well studied in structural dynamics. Practical applications of localization have not been fully explored yet, for example, how to make use of the localization characteristic to control the vibration level of the important substructure and how to improve the sensitivity of the periodic structure with a random mistuning. Thus, further studies are needed to determine the mode localization phenomenon for spherical reticulated shells.

Acknowledgements

References

[1] Anderson, P. W.: *Absence of diffusion in certain random lattices*. Physical Review, 109 (1958), 5, 1492-1505.

[2] Bendiksen, O. O.: *Localization phenomena in structural dynamics*. Chaos, Solitons & Fractals, 11 (2000), 10, 1621-1660.

[3] Bendiksen, O. O.: *Mode localization phenomena in large space structures*. AIAA Journal, 25 (1987), 9, 1241-1248.

[4] Hodges, C. H.: *Confinement of vibration by structural irregularity*. Journal of Sound and Vibration, 82 (1982), 3, 411–424.

[5] Pierre, C., Dowell, E. H.: *Localization of vibrations by structural irregularity*. Journal of Sound and Vibration, 114 (1987), 3, 549-564.

[6] Bisegna, P., Caruso, G.: *Dynamical behavior of disordered rotationally periodic structures: A homogenization approach*. Journal of Sound and Vibration, 330 (2011), 11, 2608–2627.

[7] Cornwall, P. J., Bendiksen, O. O.: *Numerical study of vibration localization in disordered cyclic structures*. AIAA Journal, 30 (1992), 2, 473-481.

[8] Cornwall, P. J., Bendiksen, O. O.: *Localization of vibrations in large space reflectors*. AIAA Journal, 27 (1989), 2, 219-226.

[9] Chan, H. C., Liu, J. K.: *Mode localization and frequency loci veering in disordered engineering structures*. Chaos, Solitons & Fractals, 11 (2000), 10, 1493-1504.

[10] Andrianov, I. V., Danishevs'kyy V. V., Kalamkarov A.L.: *Vibration localization in one-dimensional linear and nonlinear lattices: discrete and continuum models*. Nonlinear Dynamics, 72 (2013), 1-2, 37-48.

[11] Zhi, X., Fan, F., Shen S.: *Elasto-plastic instability of single-layer reticulated shells under dynamic actions*. Thin-Walled Structures, 48 (2010), 10-11, 837–845.

[12] Li, Q. S., Chen, J. M.: *Nonlinear elastoplastic dynamic analysis of single-layer reticulated shells subjected to earthquake excitation*. Computers and Structures, 81 (2003), 4, 10-11 177–188.

[13] Lopez, A., Puente, I., Serna, M. A.: *Numerical model and experimental tests on single-layer latticed domes with semi-rigid joints*. Computers and Structures, 85 (2007), 7-8, 360–374.

[14] Chen, S., in: *Matrix Perturbation Theory in Structural Dynamic Design*, Science Press, Beijing, 2007 (in Chinese).

[15] Cazin, D., Braut, S., Zigulic, R.: *Fatigue life analysis of the damaged steam turbine blade*, Engineering Review, 29 (2013), 2, 33-43.